ASC 2018 - Paper Number: 116

Title: **A Benchmark Example for Delamination Propagation Predictions Based on the Single Leg Bending Specimen under Quasi-static and Fatigue Loading**

Authors: **Ronald Krueger**[1]
Lyle Deobald[2]
Haozhong Gu[3]

[1]National Institute of Aerospace, Hampton, Virginia, USA

[2]The Boeing Company, Seattle, Washington, USA

[3]The Boeing Company, St. Louis, Missouri, USA

(FIRST PAGE OF ARTICLE – *align this to the top of page – leave space blank above ABSTRACT*)

ABSTRACT

Benchmark examples based on Single Leg Bending (SLB) specimens with equal and unequal bending arm thicknesses were used to assess the performance of delamination prediction capabilities in finite element codes. First, the development of the quasi-static benchmark cases using the Virtual Crack Closure Technique (VCCT) is discussed in detail. Second, based on the quasi-static benchmark results, additional benchmark cases to assess delamination propagation under fatigue loading are created. Third, the application is demonstrated for the commercial finite element code Abaqus Standard 2018. The benchmark cases are compared to results obtained from VCCT-based, automated quasi-static propagation analysis. A comparison with results from automated fatigue propagation analysis was not performed at this point since the current version of Abaqus does not include this capability under variable mixed-mode conditions. In general, good agreement between the results obtained from the quasi-static propagation analysis and the benchmark results were achieved. Overall, the benchmarking procedure proved valuable for analysis verification.

INTRODUCTION

Over the past two decades, the use of fracture mechanics has become common practice to characterize the onset and growth of delaminations [1, 2]. In order to predict delamination onset or propagation, the calculated strain energy release rate components are compared to interlaminar fracture toughness properties measured over a range from pure mode I loading to pure mode II loading [2].

The virtual crack closure technique (VCCT) is widely used for computing energy release rates based on results from continuum (2D) and solid (3D) finite element (FE) analyses and to supply the mode separation required when using the mixed-mode fracture criterion [3, 4]. As new VCCT-based methods for analyzing composite delamination and automated propagation analysis are incorporated into finite element codes, the need for comparison and VCCT-based benchmarking becomes important, since each code requires specific input parameters unique to its implementation.

An approach for assessing the mode I and mixed-mode I and II VCCT-based delamination propagation capabilities in commercial finite element codes under static

loading was recently presented and demonstrated for ABAQUS/Standard® [5]. The approach was then extended to allow the assessment of the delamination growth prediction capabilities under fatigue in commercial finite element codes [6]. This approach was similar to the static case. First, benchmark results were created manually using the VCCT implementation in Abaqus. Second, using the VCCT-based automated propagation analysis, a delamination in a finite element model was allowed to propagate. In general, good agreement between the results obtained from the FE propagation analysis and the benchmark results could be achieved when the appropriate input parameters were selected.

The objective of the present study is to create new benchmark examples based on the Single Leg Bending Specimen (SLB) [7] shown in Figure 1 and demonstrate the use of these benchmark cases to assess the performance of automated crack propagation prediction capabilities in Abaqus Standard 2018 [8]. These capabilities are VCCT-based and allow crack propagation between two user defined surfaces into a predefined zone of initially tied, coincident node-pairs which get successively released [8]. The SLB specimen allows variation of the mode ratio G_{II}/G_T by altering the thicknesses t_1 and t_2 of the arms. Unlike previously published benchmark cases [5], in the SLB specimen, the mode ratio is also dependent on the delamination length a. This crack length dependence provides an additional challenge to analysis codes with automated delamination propagation capabilities. Simply implementing a criterion in which propagation depends on a fixed critical energy release rate, G_c, is not sufficient in this case. Benchmarking therefore must be used to assess the appropriate implementation of mixed-mode failure criteria in finite element codes intended to be used for automated crack propagation analyses under quasi-static and fatigue loading.

In the paper, the development of benchmark cases with identical and different arm thicknesses, t_1 and t_2, is presented. First, the development of new VCCT-based benchmark cases for crack propagation prediction under quasi-static loading is discussed in detail. Second, based on the quasi-static benchmark results, additional benchmark cases to assess delamination propagation under fatigue loading are created. Third, the application is demonstrated for the commercial finite element code Abaqus Standard 2018. Results obtained from VCCT-based, automated quasi-static propagation analysis are compared to the benchmark cases. A comparison with results from automated fatigue propagation analysis was not performed at this point since the current version of Abaqus does not include this capability under variable mixed-mode conditions. Lastly, the significance of the results is discussed.

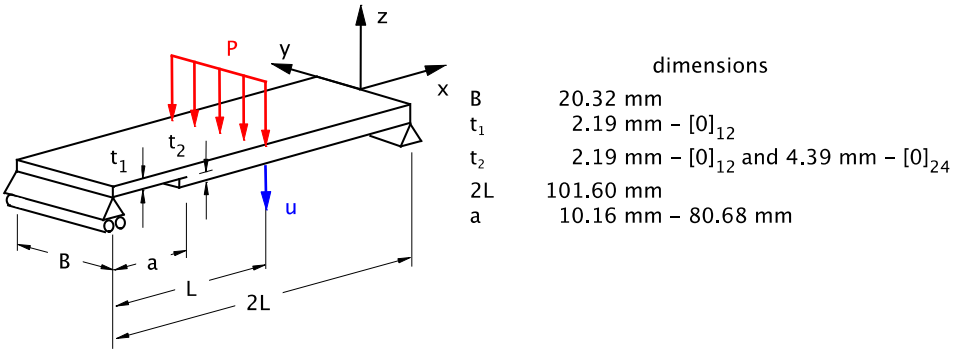

Figure 1.Single-Leg Bending (SLB) specimen.

ANALYSIS BENCHMARKING

In a previous study, the development of VCCT-based benchmark examples for delamination growth prediction under cyclic loading was presented in detail [5]. This approach was then extended to allow the assessment of the delamination growth prediction capabilities under fatigue in commercial finite element codes [6]. The examples were based on two-dimensional (2D) and three-dimensional (3D) finite element models of the Double Cantilever Beam (DCB), End-Notched Flexure (ENF) and Mixed-Mode Bending (MMB) specimens. All benchmark examples were designed to be independent of the analysis software used and allow for the assessment of the delamination growth prediction capabilities in commercial finite element codes.

Benchmark Cases for Delamination Growth Predictions Under Mixed-Mode I/II Conditions Based on the Single-Leg Bending Specimen

To allow further assessment, new benchmark examples were created for delaminations under mixed-mode conditions. For the current numerical investigation, the Single-Leg Bending (SLB) specimen, as shown in Figure 1, was chosen, since it allows variation of the mode ratio G_{II}/G_T by altering the thicknesses t_1 and t_2 of the arms. Unlike previously published benchmark cases [5], in the SLB specimen, the mode ratio is also dependent on the delamination length a, which provides an additional challenge to analysis codes with automated delamination propagation capabilities.

FINITE ELEMENT MODEL

For the current study, SLB specimens made of IM7/8552 graphite/epoxy were modeled with identical and different arm thicknesses, t_1 and t_2,. The material properties were taken from a previous study [5]. An example of the 2D finite element model of the SLB specimens with boundary conditions is shown in Figure 2a for the symmetric case ($t_1 = t_2$) and in Figure 2b for the unsymmetric case ($t_2 = 2\ t_1$).

Based on previous experience [5], the specimen was modeled with solid plane strain elements (CPE4I) in Abaqus 2018 [8] to create the benchmark cases. The SLB specimen was modeled with six elements through the specimen thickness. Along the length, all

models were divided into different sections with different mesh refinements. The resulting element lengths at the delamination tip were Δa=0.5 mm. Additional models with element length at the delamination tip of Δa=2.0 mm, 1.0 mm and 0.25 mm were also created to study the effect of mesh density on results from the automated propagation analysis.

An example of a 3D finite element model of the SLB specimen is shown in Figure 3. Through the thickness, the 3D mesh was identical to the one described above for the 2D model. Along the length and across the width, a uniform mesh with a 1mm x 1mm element size, as shown in Figure 3a, was used to avoid potential problems at the transition between a coarse and finer mesh. The specimen was modeled with solid brick elements (C3D8I), which had yielded excellent results in previous studies [5]. Additional models were created in which the element edges did not align with the advancing delamination front, as shown in Figure 3b. This intentional misalignment was created as an extra challenge for the automated propagation analysis. It is expected that in more complex, large scale problems where delamination initiation, size and shape are unknown, it will not be possible to a priori align the mesh with the propagating front. It was thus deemed appropriate to evaluate the performance of a code for non-aligned meshes. Additional models with element lengths at the delamination tip of Δa= 0.5 mm were also created to study the effect of mesh density on results from the automated propagation analysis.

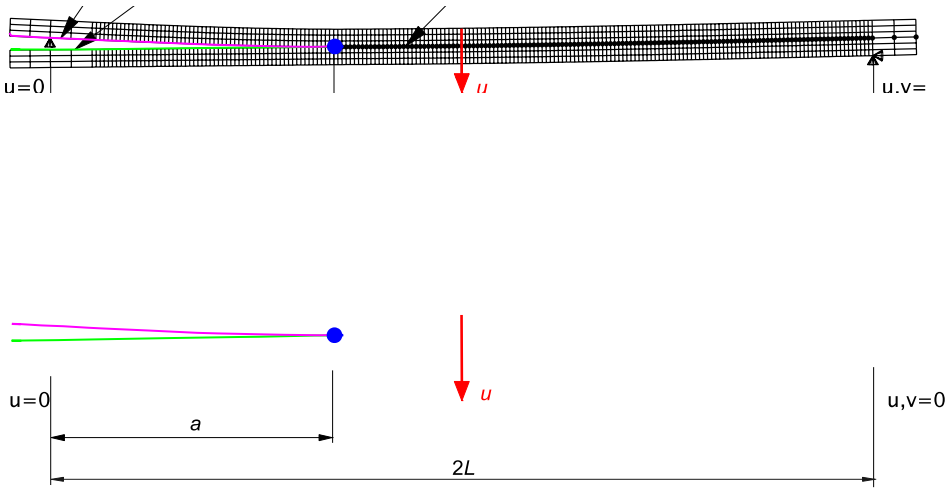

Figure 2.Two-dimensional finite element models of SLB specimens (Δa=0.5 mm).

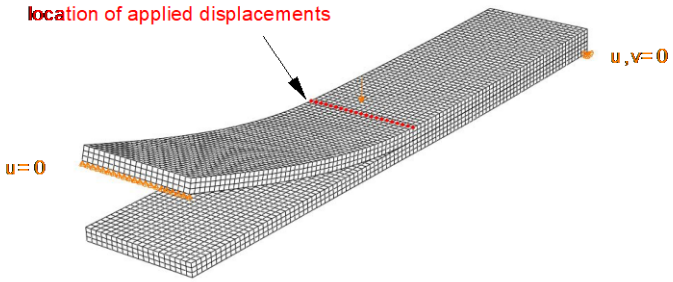

(a). *3D FE model of symmetric SLB specimen (t_1 = 2.19 mm, t_2 = 4.39 mm).*

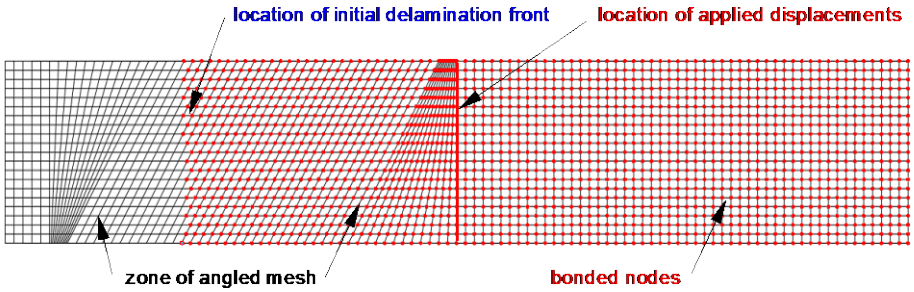

(b). *Top view of 3D FE model with angled mesh.*

Figure 3.Three-dimensional finite element models of SLB specimens (Δa=1.0 mm).

DEVELOPMENT OF BENCHMARK CASES FOR DELAMINATION GROWTH PREDICTIONS UNDER QUASI-STATIC LOADING CONDITIONS

Single-Leg Bending Specimen with Equal Arm Thicknesses

Quasi-static benchmark results can easily be created for any FE analysis software used. The procedure is discussed in detail in a paper on benchmark creation [5] and is condensed here for brevity.

- First, finite element models of the specimen with different delamination lengths, a_0, were created. For the current example, two-dimensional finite element models simulating the SLB specimen were created with 19 different delamination lengths a_0 (10.16 mm$\leq a_0 \leq$80.68 mm).
- For each delamination length, a_0, modeled, the load, P, and center deflection, u, at the load point were plotted as shown in Figure 4, where each thin solid black line represents a different value of a_0.
- For each delamination length, a_0, modeled, the total strain energy release rate, G_T, and the mixed-mode ratio G_{II}/G_T were computed using VCCT for an applied center deflection u =1.0 mm. In the current case, the mixed-mode ratio is a function of the delamination length, a_0, as shown in Figure 5 (solid blue circles). A closed-form solution developed by Davidson [7] for data reduction yielded a constant value G_{II}/G_T =0.43 independent of the delamination length which was included in the plot for comparison (dashed grey line).
- For each delamination length, a_0, modeled, a failure index, G_T/G_c, was calculated by comparing the computed total energy release rate, G_T, with the mixed-mode fracture toughness, G_c, of the material, often computed as a function of the mixed-

mode ratio. When obtaining the benchmark, G_c should be determined using the same expression for G_c used later in the automated analysis. In the present study, the B-K criterion, suggested by Benzeggah and Kenane [9], was used. It is assumed that the delamination propagates when the failure index reaches unity.

- Therefore, the critical load, P_{crit}, and critical opening displacement, u_{crit}, can be calculated based on the relationship between load, P, and the energy release rate, G,

$$\frac{G_T}{G_c} = \frac{P^2}{P_{crit}^2} \Rightarrow P_{crit} = P\sqrt{\frac{G_c}{G_T}}; \text{ and } \frac{u_{crit}}{2} = \frac{u}{2}\sqrt{\frac{G_c}{G_T}} \quad (1)$$

- For each delamination length, a_0, modeled, the critical load/displacement results were calculated using equation (1) and were included in the load/displacement plots as shown in Figure 4 (solid black circles).
- These critical load/displacement results indicated that, with increasing delamination length, less load is required to extend the delamination. For the first ten delamination lengths, a_0, investigated, the values of the critical displacements also decreased at the same time. This means that the symmetric SLB specimen exhibits unstable delamination propagation under load control as well as displacement control in this region. The remaining critical load/displacement results pointed to stable propagation.
- From these critical load/displacement results (dashed thin black line and solid circles), a benchmark solution (solid red line) can be created as shown in Figure 4. If the analysis is performed under displacement control (prescribed nodal displacements, u), the applied displacement must be held constant over several increments once the critical point (P_{crit}, u_{crit}) is reached, and the delamination front is advanced during these increments. Once the critical path is reached, the applied nodal displacement is increased again incrementally.

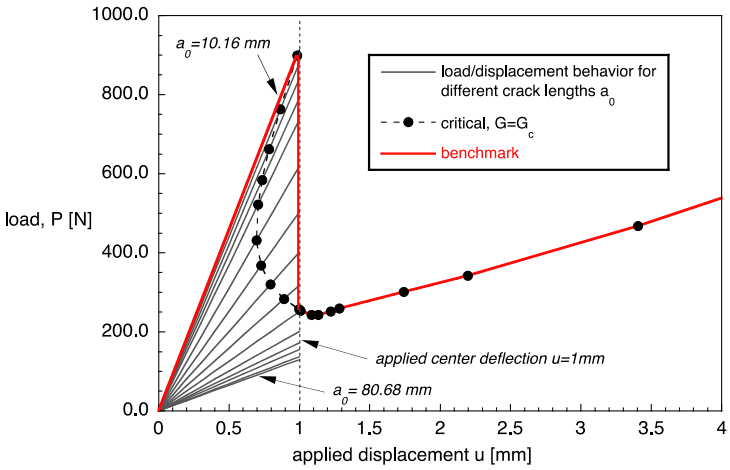

Figure 4. Computed load-displacement behavior of a symmetric SLB specimen for different delamination lengths a_0, calculated critical behavior and resulting benchmark case.

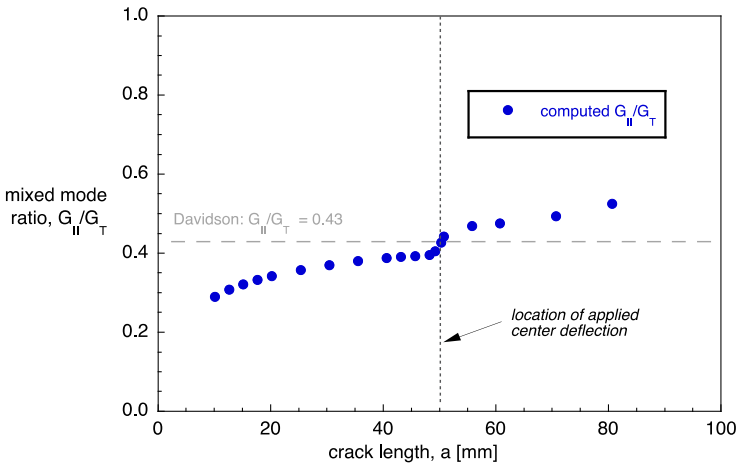

Figure 5.Computed mixed-mode ratio for different delamination lengths a_0 for a symmetric SLB specimen.

During the automated propagation analysis, the computed load/displacement results are expected to follow the benchmark solution (solid red line). Throughout the development and application of the benchmark examples, it was assumed that the delamination front remained straight for each delamination length, a_0, modeled. In reality, a delamination develops into a somewhat curved front during propagation. This, however, was not considered for the current benchmarking exercise.

Single-Leg Bending Specimen with Unequal Arm Thicknesses

The procedure outlined above was repeated for the unsymmetric SLB specimen. The computed load/displacement results for the specimens with different delamination lengths a_0 (thin solid black lines), the calculated critical behavior (dashed line and solid black circles) and the resulting benchmark case (solid red line) are shown in Figure 6. If the analysis is performed under displacement control (prescribed nodal displacements, u) the applied displacement must be held constant over several increments once the critical point (P_{crit}, u_{crit}) is reached, and the delamination front is advanced during these increments. Once the critical path is reached, the applied nodal displacement is increased again incrementally.

For the chosen configuration of the unsymmetrical SLB specimen, the mixed-mode ratio is a function of the delamination length, a_0, as shown in Figure 7 (solid blue circle). A closed form solution developed by Davidson [7] for data reduction yielded a constant value G_{II}/G_T =0.38 independent of the delamination length which was included in the plot for comparison (dashed grey line).

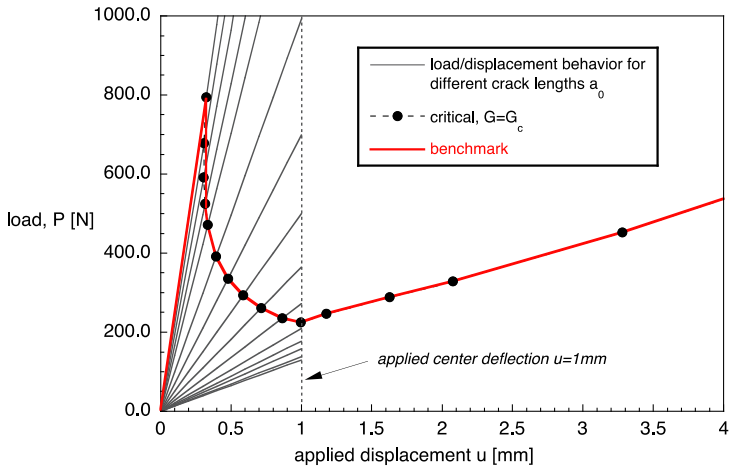

Figure 6. Computed load-displacement behavior of an unsymmetrical SLB specimen for different delamination lengths a_0, calculated critical behavior and resulting benchmark case.

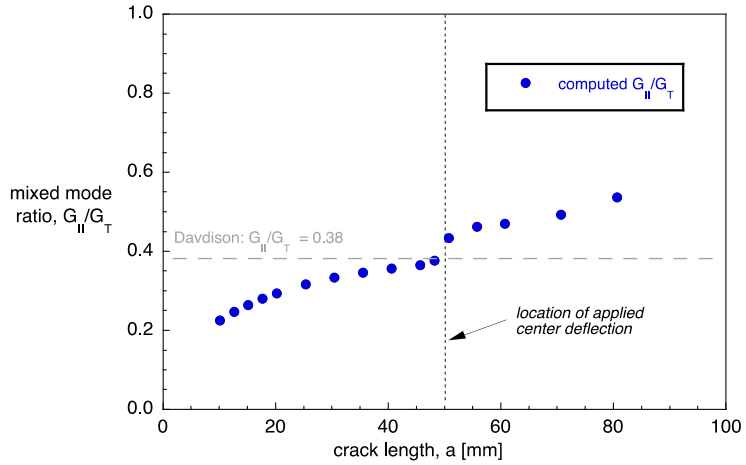

Figure 7.Computed mixed-mode ratio for different delamination lengths a_0 for an unsymmetrical SLB specimen.

Development of Benchmark Cases for Delamination Growth Predictions Under Cyclic Loading Conditions (Fatigue)

The fatigue benchmark problem for the SLB specimen is developed as an extension of the static benchmark results. Fatigue load levels were chosen at 40%, 50%, 60% and 70% of the static critical load, G_c, and this corresponds to target displacements of 63%, 71%, 77%, 84% of the critical delamination onset displacement, u_{crit}. The applied constant displacement was based on the critical load for the initial crack length. However, the crack tip criticality changes as a function of crack length. Consequently, the crack tip may have sections of intermittent static crack growth and damage arrestment. The SLB benchmark demonstrates this behavior. Interlaminar crack growth behavior will depend on mode mix, stress ratio and R-curve effects [11]. Because mixed-mode crack growth rates from SLB specimens are currently not available, these crack growth rates must be interpolated from existing data. Thus, the mixed-mode crack growth rates may be characterized with the Mixed-Mode Bend (MMB) test [12] under cyclic loading. Ratcliffe, et al [13] provided MMB crack growth rates for IM7/8552 CFRP material for 20%, 50% and 80% G_{II}/G_T mode mix that were used in the fatigue

calculations presented here. Considering the various forms in which crack growth rate data may be published for various materials, a convenient interpolation scheme is necessary to calculate crack growth rates for a crack tip under arbitrary loading.

Reference 11 performed a light review of various mode mix interpolation schemes for interlaminar fatigue delamination growth. Data plotted in log-log space resulted in a linear (region II) Paris Law in the crack growth rates of practical range. Reference 11 also discussed the nonlinear regions I and III as crack growth rates transitioned to the threshold value and the critical value, respectively. The mixed mode interpolation was not always intuitive. A practical means to deal with the uncertainty of characterizing the crack growth rate for intermediate mode mix is to characterize the crack growth rate behavior using the MMB test [12] as described in Reference 13 and then input the measured crack growth rate data in tabular form into an interlaminar fatigue analysis code. Figure 8 shows the notional tabular data for 0%, 50% and 100% G_{II}/G_T.

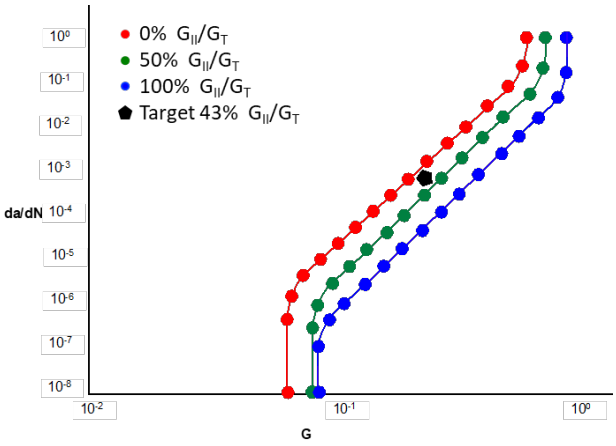

Figure 8. Notional mixed-mode crack growth data.

Consider the task of determining a crack growth rate for 43% G_{II}/G_T mode mix ratio (MMR) given measured data at discrete mode mix ratios. The first step is to convert crack growth data into Log-Log space where x=log(G_T) and y=log(da/dN). Given sufficient measured crack growth data for various mode mix ratios, a linear interpolation scheme will be adequate to determine the crack growth rate for an intermediate mode mix ratio and energy release rate. Figure 9(a) shows four measured crack growth rate data points (yellow circles) which can be used to determine the crack growth rate associated with the targeted intermediate mode mix and energy release rate (red circle). The first step in Figure 9(a) was to interpolate to a constant targeted mode mix line $MMR=G_{II}/G_T$=0.43. Equations in Figure 9(a) calculate the intermediate mode mix line (blue circles) based on the targeted MMR and the known bounding mode mix ratios, $MMR_{(-)}$ and $MMR_{(+)}$. The final step shown in Figure 9(b) interpolates along the constant MMR line to a value associated with the targeted total energy release rate x_{MMR}=log(G_T). The equation in Figure 9(b) yields a value y_{MMR} that is converted to the crack growth rate, $da/dN_{MMR}=10^{y_{MMR}}$, associated with crack tip loading, G_T.

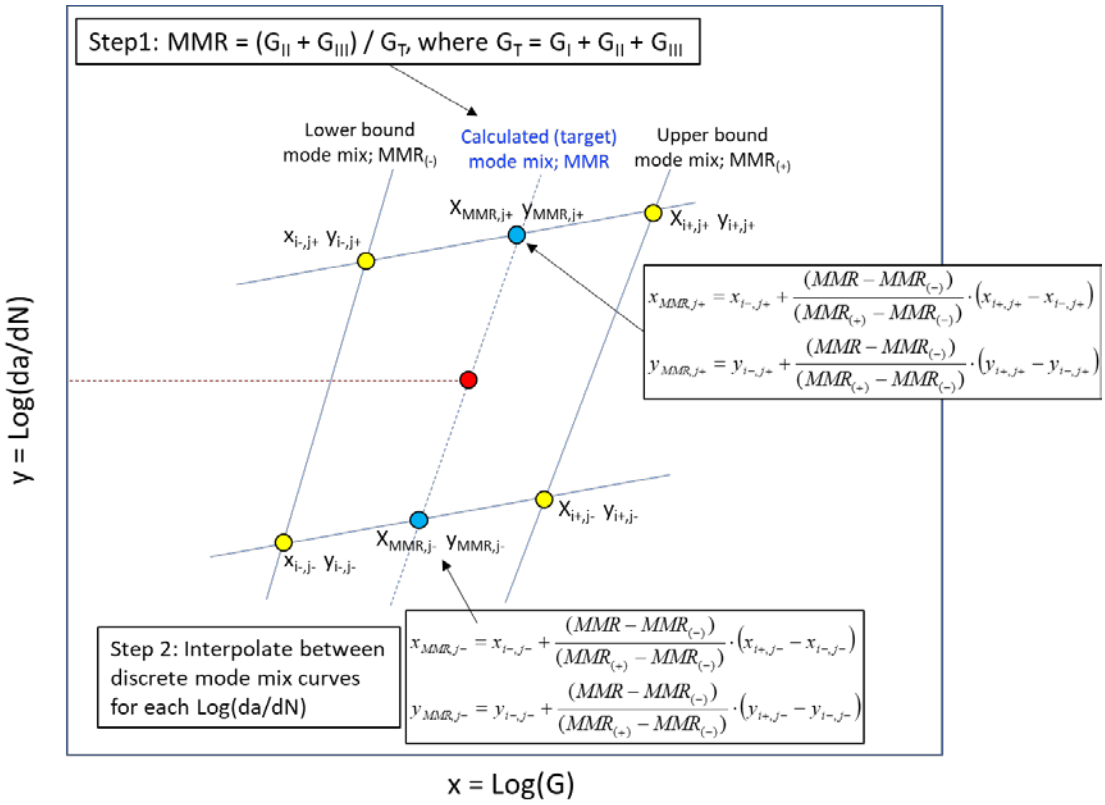

(a)

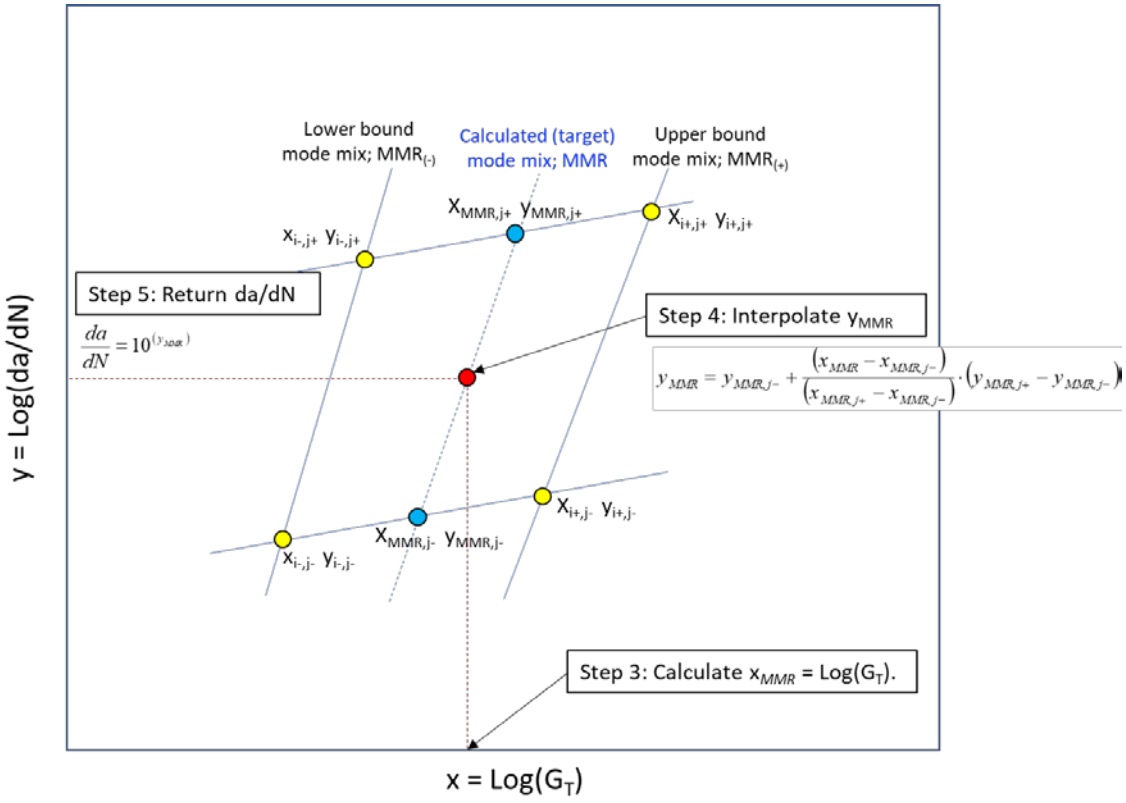

(b)

Figure 9. Mode mix interpolation scheme based on tabular inputs of crack growth data.

The critical energy release rates from the static benchmark simulation of Figure 4 were used to calculate the fatigue crack growth history in Figure 10 based on the mixed-mode Paris Laws characterized in Ref. 13. Figure 10(a) shows fatigue calculations based on a 43% G_{II}/G_T mode mix and Figure 10(b) shows the same calculations using the VCCT based mode mix from Figure 5. The graphs show similar crack growth behavior, however, the assumption of constant 43% mode mix under predicts the damage. Both simulations show a segment of unstable static growth for the 60% and 70% G/G_c load levels and the variable mode mix (Figure 10(b)) shows a longer static jump. This behavior is expected since the variable mode mix simulation will have higher mode I loading for crack lengths that have not reached the center load point (see Figure 5). All simulations show fatigue crack arrestment in the crack length range of 42 to 48 mm. These results will serve as benchmark fatigue cases and will be used to evaluate future automated interlaminar fatigue delamination codes.

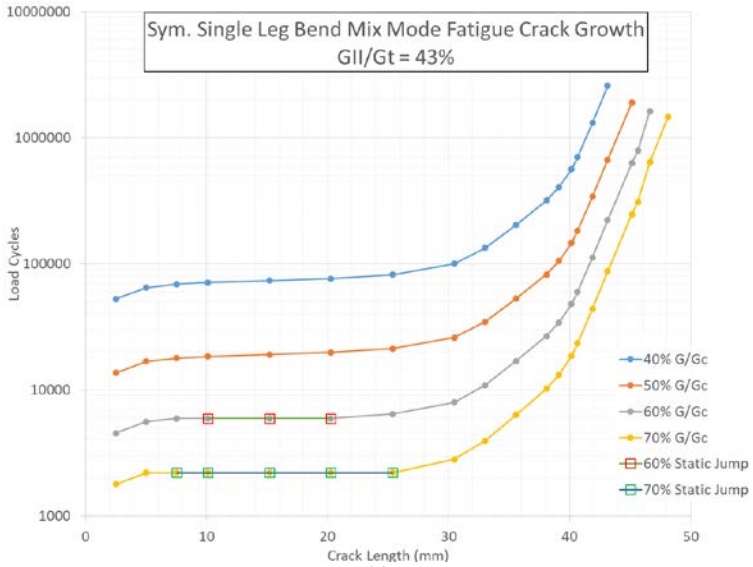

(a)

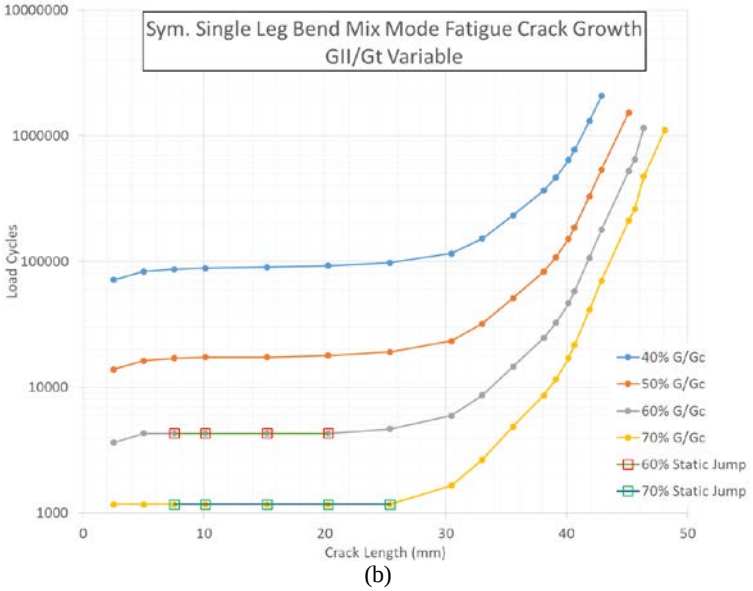

(b)

Figure 10. Crack growth history for assumed constant G_{II}/G_T=0.43 (a) and variable mode ratio from Figure 5.

ASSESSMENT OF RESULTS FROM AUTOMATED GROWTH ANALYSES

In the present section, the application of the benchmark is demonstrated and the delamination prediction capabilities implemented in Abaqus Standard 2018 are assessed using the symmetric and unsymmetric SLB benchmark cases developed above. The effect of four different crack tip element sizes Δa (Δa= 2mm, 1 mm, 0.5 mm, 0.25 mm) on automated crack propagation results was investigated.

In Abaqus Standard, a user specified release tolerance parameter is used to improve the accuracy of the VCCT-based local solution [8]. If this release tolerance is exceeded in an increment ($(G-G_c)/G_c > release\ tolerance$), a cutback operation is performed which reduces the time increment. In the new smaller increment, the strain energy release rates are recalculated and compared to the user specified release tolerance. A release tolerance, *reltol*=0.2, is suggested in the handbook [8]. However, a tighter tolerance should be used to achieve better accuracy. For the current analysis, a tighter tolerance, *reltol*=0.01, was chosen. Another parameter, which Abaqus Standard provides to help overcome convergence issues during the propagation analysis, is *contact stabilization*, which is applied only across selected contact pairs and used to control the motion of two contact pairs while they approach each other in multi-body contact. Damping is applied when bonded contact pairs debond and move away from each other [8]. For the current analysis, a stabilization factor equal to 10^{-6}, which had yielded good results in previous analyses [5], was chosen. Excessive stabilization may adversely affect the predicted load levels.

To simulate the propagation of cracks, the element at the crack tip may either be completely released once the fracture criterion is reached or released gradually. Abaqus offers the complete release using the option *debonding force=step* [8]. The gradual release is used to represent intermediate crack positions between existing node pairs. Using this approach, the nodes are allowed to be released progressively rather than suddenly and the forces are ramped down accordingly. Abaqus offers this approach using the option *debonding force=ramp* [8]. Both approaches were used in the current study. More detailed information about VCCT with progressive nodal release can be found in a related paper [10].

The propagation analysis in Abaqus was performed in two steps starting from an initial delamination length, a_0=10.16 mm. In the first step, a center deflection of 80% u_{crit} (u=0.8 mm) was applied to the model so that the region of linear load/displacement behavior could be analyzed quickly. During this first step, large displacement increments were allowed and automated propagation was disabled. In the second step, the center deflection was increased from u=0.8 mm to u=4.0 mm. Automated propagation was enabled, the B-K criterion for mixed-mode failure was selected and the limit for the smallest increment size was set equal to 10^{-20} to reduce the risk of numerical instability and early termination of the analysis and allow for sufficient cut-back during the propagation phase of the analysis.

Single-Leg Bending Specimen with Equal Arm Thicknesses

Example results using Abaqus Standard 2018 (first release) are shown in Figures 11 through 13 where the computed resulting load (load P) at the center of the SLB specimen (Figure 1) is plotted versus the applied center deflection (u) for different crack tip element sizes Δa. For all 2D element sizes studied, the computed load slightly

exceeded the critical point before the initial load drop occurred and delamination propagation started (colored solid lines), as shown in Figure 11. As desired, the load continued to drop after reaching the peak load and the computed load/displacement path converged to the stable propagation branch of the benchmark result (solid black line). When the coarse mesh (Δa = 2 mm) was used in combination with the *step option* in Abaqus, a saw-tooth pattern was observed once the stable path was reached in the analysis where the peaks of the saw-tooth were in good agreement with the benchmark case (solid red line). The results closely followed the benchmark when the *ramping option* was used in Abaqus (solid blue line). Only a small saw-tooth pattern was observed for the other cases, due to the finer meshes used($\Delta a \leq 1$ mm). These results confirm the observations made in previous studies [4-6] with respect to input parameter settings for release tolerance and contact stabilization.

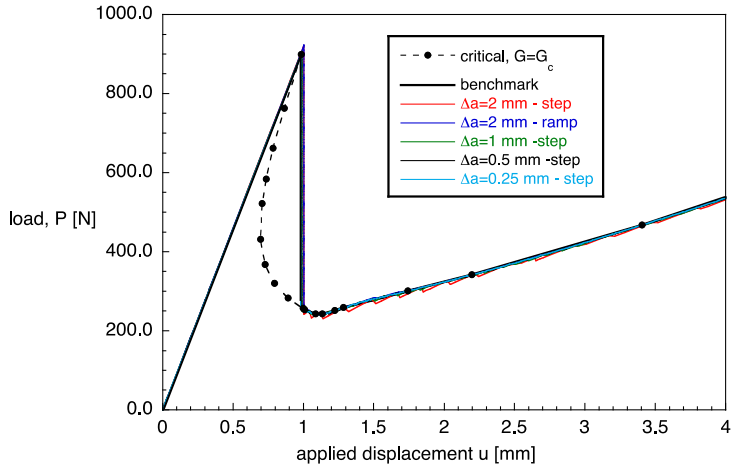

Figure 11. Computed load-displacement results obtained from automated propagation analyses of a symmetric SLB specimen using 2D FE models.

The results from 3D models with aligned, straight meshes are shown in Figure 12. For the element sizes studied, the computed load and displacement slightly exceeded the critical point before the initial load drop occurred and delamination propagation started (red and blue lines) as shown in Figure 12.

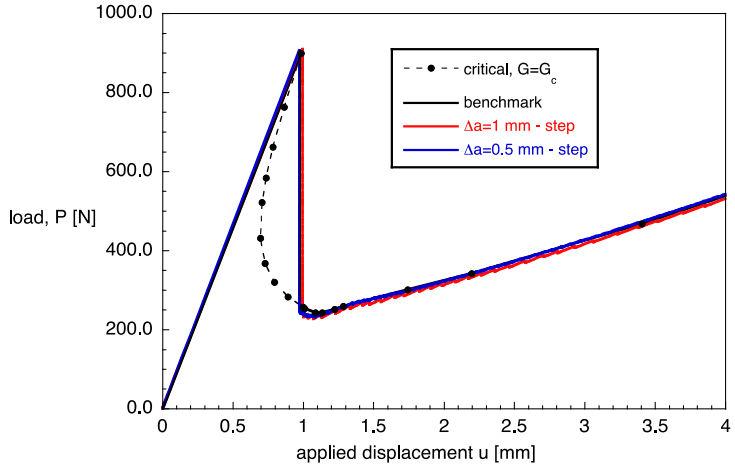

Figure 12. Computed load-displacement results obtained from automated propagation analyses of a symmetric SLB specimen using 3D FE models with aligned, straight meshes.

As desired, the load dropped at the critical point and closely followed the benchmark result (solid black line) during the phase of unstable crack growth. The computed results dropped slightly below the benchmark before again converging to the stable propagation branch of the benchmark result (solid black line). Once the stable path is reached in the analysis, when the coarse mesh (Δa = 1 mm) was used in combination with the *step option* in Abaqus, a saw-tooth pattern was observed where the peak results are in good agreement with the benchmark case (solid red line). Only a small saw-tooth pattern was observed for the other case (Δa =0.5 mm), due to the finer mesh.

The results from 3D models with misaligned, angled meshes are shown in Figure 13. Regardless of the mesh size, delamination propagation started prematurely when the *step option* in Abaqus was used during the analysis (red and blue lines) as shown in Figure 13. This premature delamination propagation is caused by a premature node release due to computed spikes in the energy release rate at corner nodes along the zig-zag shaped misaligned front. The results closely followed the benchmark when the *ramping option* was used in Abaqus (solid green and orange lines). The results highlight the importance of progressive nodal release, the details of which are discussed in a related study [10].

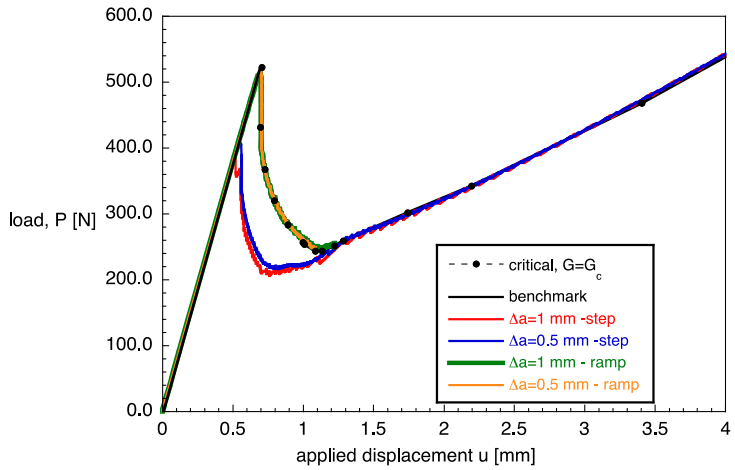

Figure 13. Computed load-displacement results obtained from automated propagation analyses of a symmetric SLB specimen using 3D FE models with misaligned, angled meshes.

Single-Leg Bending Specimen with Unequal Arm Thicknesses

Example results using Abaqus Standard 2018 are shown in Figures 14 through 16 where the computed resulting load (load P) at the center of the unsymmetric SLB specimen (Figure 1) is plotted versus the applied center deflection (u) for different crack tip element sizes Δa. As for the symmetric cases, the computed load and displacement slightly exceeded the critical point before the initial load drop occurred and delamination propagation started (colored solid lines), as shown in Figure 14 for all 2D element sizes studied. As desired, the load continued to drop after reaching the peak load and the computed load/displacement path converged to the stable propagation branch of the benchmark result (solid black line). When the coarse mesh (Δa = 2 mm) was used in combination with the *step option* in Abaqus, a saw-tooth pattern was observed once the stable path was reached in the analysis where the peak results were in good agreement with the benchmark case (solid red line). The results closely followed

the benchmark when the *ramping option* was used in Abaqus (solid blue line). Due to the finer meshes, only a small saw-tooth pattern was observed for the other cases ($\Delta a \leq$ 1 mm). These results confirm the observations made in previous studies [4-6] with respect to input parameter settings for release tolerance and contact stabilization.

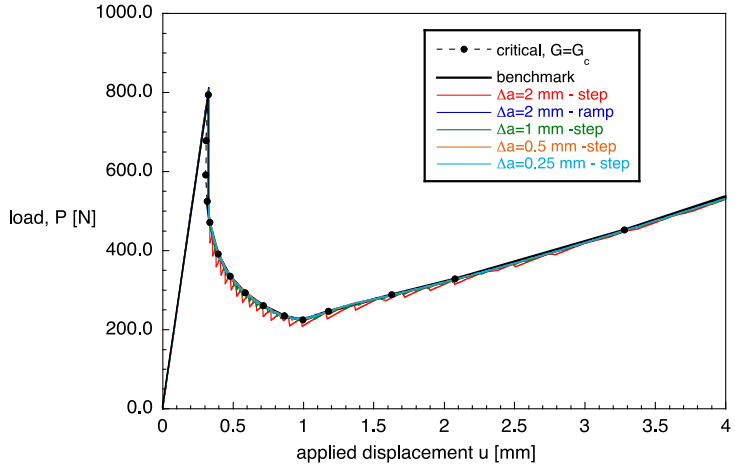

Figure 14. Computed load-displacement results obtained from automated propagation analyses of an unsymmetric SLB specimen using 2D FE models.

The results from 3D models with aligned, straight meshes are shown in Figure 15. For the element sizes studied, the computed load and displacement slightly exceeded the critical point before the initial load drop occurred and delamination propagation started (red and blue lines) as shown in Figure 15.

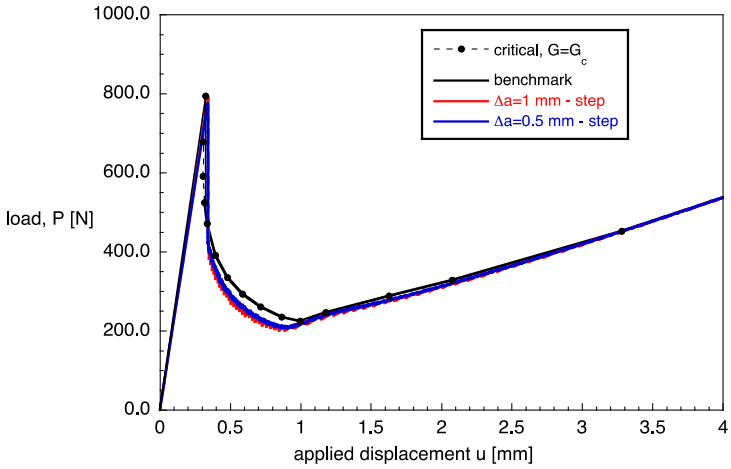

Figure 15. Computed load-displacement results obtained from automated propagation analyses of an unsymmetric SLB specimen using 3D FE models with aligned, straight meshes.

As desired, the load continued to drop after reaching the peak load and the computed load/displacement path closely followed the benchmark result (solid black line) during the phase of unstable crack growth. The computed results dropped slightly below the benchmark before again converging to the stable propagation branch of the benchmark result (solid black line). Once the stable path is reached in the analysis, a saw-tooth pattern (solid red line) was observed where the peak results are in good agreement with the benchmark case when a coarse mesh (Δa = 1 mm) was used in combination with the *step option* in Abaqus. Due to the finer mesh, only a small saw-tooth pattern was

observed for the other case (Δa =0.5 mm). Results following closer to the benchmark might be obtained from analyses in combination with the *ramp option* in Abaqus.

The results from 3D models with misaligned, angled meshes are shown in Figure 16. Regardless of the mesh size, delamination propagation started prematurely when the *step option* in Abaqus was used during the analysis (red and blue lines) as shown in Figure 16. This premature delamination propagation is caused by a premature node release due to computed spikes in the energy release rate at corner nodes along the zig-zag shaped misaligned front (see Figure 3c).

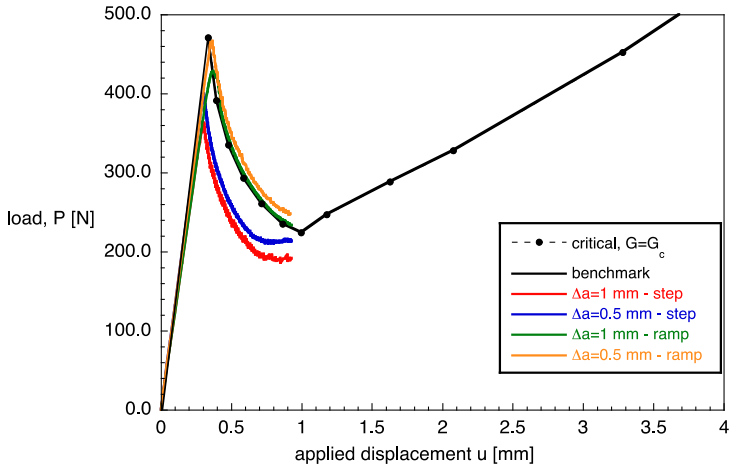

Figure 16. Computed load-displacement results obtained from automated propagation analyses of an unsymmetric SLB specimen using 3D FE models with misaligned, angled meshes.

The results closely followed the benchmark when the *ramping option* was used in Abaqus (solid green and orange lines). The analyses were terminated when the applied displacements reached u =1 mm. At this point in the analyses, the delamination had propagated into an area with an irregular element size where the mesh transitions from a misaligned to an aligned, straight mesh (see Figure 3c). Thus, the analyses should be repeated with a more regular mesh. The results highlight the importance of progressive nodal release, the details of which are discussed in a related study [10].

In general, the examples shown highlight the importance of benchmarking to identify critical analysis input parameters. In summary, good agreement between the load-displacement relationship obtained from the propagation analysis results and the benchmark results could be achieved by selecting the appropriate input parameters, such as ramping, for misaligned, angled meshes. Since the change of mixed-mode ratio with crack length did not create any observable problem during automated propagation, it may be concluded that the mixed mode B-K criterion was implemented correctly.

SUMMARY AND CONCLUSIONS

The development of VCCT-based benchmark examples used to assess the performance of quasi-static and fatigue delamination prediction capabilities in finite element codes was shown in detail for Single Leg Bending (SLB) specimens with equal and unequal bending arm thicknesses. The application was subsequently demonstrated for automated quasi-static propagation analysis using the commercial finite element code Abaqus Standard 2018. A comparison with results from automated fatigue propagation analysis was not performed at this point since the current version of Abaqus does not include this capability under variable mixed-mode conditions.

First, quasi-static VCCT-based benchmark results were obtained. Differing from previously published benchmark cases, a dependence of the mixed-mode ratio on the delamination length was observed. This crack length dependence provided an additional challenge to the analysis code with automated delamination propagation capabilities. For both the benchmark creation and the automated propagation analysis the B-K criterion were used to address the varying mixed-mode ratio. Second, based on the quasi-static benchmark results, additional benchmark cases to assess delamination propagation under fatigue loading were created. Third, the delamination was allowed to propagate under quasi-static loading from its initial location using the automated procedure implemented in Abaqus 2018. Input control parameters were varied to study the effect on the computed delamination propagation.

This study showed the following:

- The benchmarking procedure is independent of the analysis software.
- Benchmark solutions are based on Linear Elastic Fracture Mechanics (LEFM) and VCCT.
- In general, good agreement between the results obtained from the quasi-static propagation analysis and the benchmark results could be achieved by selecting the appropriate input parameters.
- For Abaqus 2018 in particular, the results for automated delamination propagation analysis under quasi-static loading showed the following:
    - Good agreement between analysis results and the benchmarks could be achieved for release tolerance values (*reltol*<0.1) in combination with contact stabilization ($cs=1x10^{-6}$). These results confirmed previous observations.
    - Progressive nodal release using the ramp option should be used to avoid the observed saw-tooth behavior during automated propagation.
    - Progressive nodal release using the ramp option must be used to obtain accurate results when the mesh is not aligned with the delamination front.

Overall, the benchmarking procedure proved valuable by highlighting the issues associated with choosing the appropriate input parameters for the VCCT implementations in Abaqus 2018. In the context of analysis *Verification and Validation* (V&V), these benchmarks may also be used for code and calculation verification purposes and thus serve as a valuable tool for software developers. Specifically, these benchmark solutions should be used to evaluate other algorithms for delamination prediction, such as cohesive elements and adaptive mesh VCCT algorithms.

Further, fatigue benchmark cases based on the unsymmetric SLB specimen should be created. Additionally, analyses are required to assess the automated delamination fatigue growth prediction capabilities in Abaqus using the developed fatigue benchmarks. Subsequently, studies are required to validate the analyses against test results obtained from more complex specimens and on a structural level.

ACKNOWLEDGEMENTS

The material is based upon work supported by NASA under Award No. NNL09AA00A.

REFERENCES

1. Tay, T. E. 2003. "Characterization and Analysis of Delamination Fracture in Composites - An Overview of Developments from 1990 to 2001," *Applied Mechanics Reviews*, 56, 1-32.
2. Raju, I.S., and T.K. O'Brien. 2008. "Fracture Mechanics Concepts, Stress Fields, Strain Energy Release Rates, Delamination and Growth Criteria," in *Delamination behaviour of composites*, Srinivasan Sridharan ed., Woodhead Publishing in Materials.
3. Rybicki, E. F., and M. F. Kanninen. 1977. "A Finite Element Calculation of Stress Intensity Factors by a Modified Crack Closure Integral," *Eng. Fracture Mech.,* 9:931-938.
4. Krueger, R. 2015. "The Virtual Crack Closure Technique for Modelling Interlaminar Failure and Delamination in Advanced Composite Materials," in *Numerical Modelling of Failure in Advanced Composite Materials*, P. Camanho and S. Hallett, eds., Woodhead Publishing Ltd., pp. 3-53.
5. Krueger, R. 2015. "A Summary of Benchmark Examples and Their Application to Assess the Performance of Quasi-Static Delamination Propagation Prediction Capabilities in Finite Element Codes," *Journal of Composite Materials* 49 (26):3297-3316.
6. Krueger, R., N. V. D. Carvalho, and M. Sasdelli. 2017. "Searching for Run-Time Efficient Approaches to Delamination Growth Predictions in Composites," in *Proceedings of NAFEMS World Congress*, Stockholm, Sweden, 2017.
7. Davidson, B.D. and V. Sundararaman. 1996. "A Single Leg Bending Test for Interfacial Fracture Toughness Determination," *International Journal of Fracture*, vol. 78, pp. 193-210.
8. Abaqus Analysis User's Guide. 2018. Abaqus 2018, DS Simulia Corp., Providence, RI, USA.
9. Benzeggagh M.L. and M. Kenane. 1996. "Measurement of Mixed-Mode Delamination Fracture Toughness of Unidirectional Glass/Epoxy Composites with Mixed-Mode Bending Apparatus," *Composites Science and Technology*; 56: 439-449.
10. Mabson, G.E. , N.V. De Carvalho and R. Krueger. 2018. "VCCT with Progressive Nodal Release for Simulating Mixed-Mode Delamination: Formulation, Algorithmic Improvements and Implications," in *Proceedings of ASC 33rd Technical Conference*, Seattle, WA.
11. Deobald, L.R., et al. 2017. "Guidelines for VCCT-Based Interlaminar Fatigue and Progressive Failure Finite Element Analysis," NASA/TM-2017-219663.
12. "ASTM D6671/D6671M-13 Standard Test Method for Mixed Mode I-Mode II Interlaminar Fracture Toughness of Unidirectional Fiber Reinforced Polymer Matrix Composites," 2013. *Annual Book of ASTM Standards.* Vol. 15.03, ASTM International..
13. Ratcliffe J.G. and W.M. Johnston. 2014. "Influence of Mixed Mode I-Mode II Loading on Fatigue Delamination Growth Characteristics of a Graphite Epoxy Tape Laminate," in *Proceedings of American Society for Composites 29th Technical Conference*, San Diego, CA.